

Pressure Measurements on Full-Scale and Model-Scale Upwind Sails I.M. Viola¹, E. Gauvain¹ and R.G.J. Flay¹

¹Yacht Research Unit, University of Auckland, Auckland 1142, New Zealand

Abstract

The pressure distribution on upwind sails was investigated both with model-scale pressure tapped sails in a wind tunnel and with full-scale sails tested on a 24-foot yacht. The present paper summarises the results of the tests describing the pressure distributions on the two sails. The flow field correlated with the pressure measurements is also discussed.

Introduction

Numerical fluid dynamic methods are widely used to investigate sail aerodynamics. Potential flow codes are used to investigate the aerodynamics in upwind conditions, when a mainsail and a genoa are sailed and the flow is mainly attached. Conversely, Reynolds Averaged Navier-Stokes codes, and more recently Large Eddy Simulations, are used to investigate the aerodynamics in downwind conditions, where the effect of separation is not negligible.

Experimental measurements on sails are typically performed in wind tunnels. It is common practice to use flexible sails, which allow the sails to be trimmed. Aerodynamic forces are typically measured with a balance attached to the model. Pressures are rarely measured. In fact, model-scale sails must be light and thin, which makes it difficult for pressure taps to be used. As far as is known by the present authors, pressure distributions on three-dimensional upwind model-scale sails have never been published. Conversely, pressure distributions on full-scale sails were measured the first time in 1925 by Warner & Ober [1] and much later in 2010 by Viola & Flay [2].

Pressure measurements are needed to validate numerical simulations. In fact, different pressure distributions can provide the same global aerodynamic force. Hence, to validate the computed pressure distribution, a pressure measurement is necessary.

In the present paper, pressure distributions on upwind sails were measured in a wind tunnel on horizontal sections of rigid pressure-tapped sails. In a previous paper [2], pressures were measured on full-scale sails tested on a 24-foot sailing yacht. The results of the large number of tests performed in both model-scale and full-scale are summarised herein and describe the general pressure distributions on the genoa and the mainsail.

Method

The Yacht Research Unit (YRU) developed an innovative pressure system capable of acquiring up to 512 channels at speeds up to 3,900 Hz on each channel. Additional details of the pressure system are provided in [2]. The system was used to measure the pressures on model-scale rigid pressure-tapped sails, which were designed for the America's Cup class "AC33". A 1/15th model-scale mainsail and genoa were built with fibreglass and sandwich structures. The core was made of a 2 mm thick polypropylene plastic sheet, which had 3 mm wide core flutes. Pressures were carried along the sail in the core-flutes to the sail foot. Pressure tubes carried the pressure from the sail foot to the transducers, which were placed in the cockpit. The sails were perforated along 5 horizontal sections. On the 5 mainsail

sections, 9, 11, 13 and 14 holes were used on the top to the bottom sections, respectively. On the 4 genoa sections, 7, 8, 11 and 15 holes were used on the top to the bottom sections, respectively. To measure the leeward side of the sail, tape was used to close the holes on the windward side, and vice versa. Additional details of the sail construction can be found in [3].

The sails were fixed onto a model-scale yacht with rigid mast, and were tested in the Twisted Flow Wind Tunnel of the YRU. The wind tunnel is an open jet with a test section 7m wide and 3.5m high.

The wind experienced by a sailing yacht, resulting from the vector difference between the atmospheric boundary layer and the yacht velocity, is called the "apparent wind". The change in direction of the apparent wind velocity with the height is called the "twist". The apparent wind angle (AWA) is the supplementary angle between the yacht velocity and the apparent wind velocity.

Four different mainsail and genoa trims, four AWAs (16°, 20°, 24° and 28°), several heel angles (from 0° to 20°) and several twists of the onset flow were tested. The pressure measurements with variations in the heel angle and the twist of the onset flow are not presented in the present paper due to the limitation in the maximum number of pages.

The reference pressure p_∞ was provided by the static tap of a Pitot-static tube, which was located roughly 6h upstream of the model (being h=2.3m the model height). The total-pressure tap of the same Pitot-static tube was used to measure the reference dynamic pressure $q_\infty = 32.5\text{Pa}$. The Reynolds number Re based on the average chord length $c=0.49\text{m}$ was $Re = 2.3 \cdot 10^5$. The pressure measurement accuracy was estimated about $\pm 0.5\text{ Pa}$.

The same pressure system was used to measure the pressure distributions on full-scale sails. Pressures from 30 and 33 pressure taps on the mainsail and genoa, respectively, of a Sparkman & Stephens 24-foot yacht (SS24) were measured. Several sail trims and apparent wind angles were tested. More details can be found in [2]. Figure 1 shows a schematic drawing of the AC33 and the SS24 sailplans.

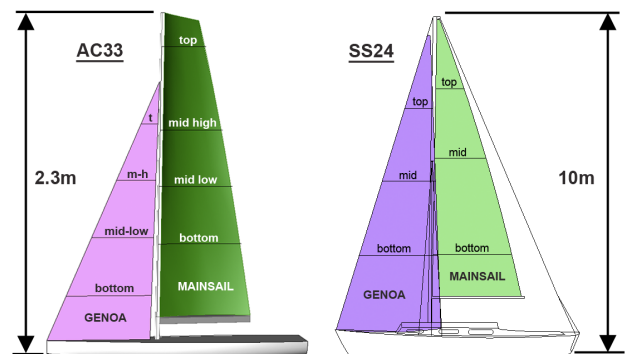


Figure 1: Layout of the AC33 and the SS24 sailplans.

In the following, the pressure distributions on the measured sail sections are correlated with the angle of attack (AoA), which results from the sail trims and the AWA.

Pressure Distribution on the Genoa

Ideal Angle of Attack

The genoa is a thin cambered profile. If the genoa is trimmed at the “*ideal angle of attack*”, the local flow is tangent to the sail at the leading edge. The stagnation point is located at the leading edge, where the pressure coefficient, defined as $C_p = (p - p_\infty) / q_\infty$, is $C_p = 1$.

Pressure Distribution on the Genoa at the Ideal AoA

On cambered sails, at the ideal AoA, an attached boundary layer grows from the leading edge. The leeward pressure distribution shows a suction peak correlated with the position of maximum camber. The pressure recovery following the suction peak can lead to trailing edge separation. In these circumstances, the mean stream velocity and the velocity gradients in the separated region are small and, hence, the pressure gradients are small. Where the separation occurs, the pressure recovery is interrupted and the pressure remains almost constant at the so-called “*base pressure*” up to the trailing edge.

Pressure Distribution on the Genoa at Low AoAs

On the leeward side of flexible genoas, when the AoA is lower than the ideal AoA, the leading edge collapses. Conversely, on rigid sails, the sail shape does not change. In this latter case, decreasing the AoA causes the camber-related suction peak to decrease, while the pressures at the trailing edge remains almost constant or increase slightly.

Leading Edge Separation Bubble

At AoAs higher than the ideal AoA, the flow separates at the sharp leading edge and a separation bubble occurs on the leeward side of the sail.

There are two types of leading-edge separation bubbles: short bubbles, which typically occur on rounded-nose conventional airfoils, and long bubbles, which typically occur on thin airfoils. The first bubble type affects the performance of airfoils and it is of particular interest in aeronautical applications. The laminar to turbulent transition occurs in the latest part of the bubble [4] and the reverse flow velocity inside the bubble is typically less than 20% of the free-stream velocity. The second leading edge bubble type became of interest in the 1950s, when high-speed aircraft adopted thin airfoils to decrease compressibility effects. The research on long bubbles increased with the turbo-machinery development, where thin blades are used, and with the growth of low-Reynolds-number aviation. The major characteristic of long leading-edge bubbles is the generation of a large recirculation region with high backflow velocity. On long bubbles, the separation occurs at the sharp leading edge. The laminar to turbulent transition occurs at the earliest part of the bubble. An investigation on laminar separation bubbles on flat plates performed at $Re = 2.13 \cdot 10^5$ [5] shows that at least 95% of the shear layer is turbulent. Consequently, the reattached flow is more energetic in the long bubble type than in the short bubble type, and the backflow in the recirculation region is significantly faster. The centrifugal force that curves the flow inside the bubble is due to a high suction peak inside the recirculation region. The backflow that decelerates near the leading edge can separate due to the high positive pressure gradient, forming a secondary separation bubble. Figure 2 shows a schematic diagram of the long leading edge bubble type.

Pressure Distribution on a Flat Plate

On flat plates, the shear layer re-attaches for AoAs lower than 5° . For $AoA \neq 0$ and inviscid flow, the stagnation point is located on the windward side. Conversely, in viscous flow, the stagnation point remains at the leading edge for a range of AoAs. In fact, [5] shows that the stagnation point remains at the leading edge for $-20^\circ < AoA < 20^\circ$.

The suction peak correlated with the recirculation flow occurs at around 30% of the bubble length. Downstream of the suction peak, the pressure increases asymptotically reaching $C_p = -0.1$ at the trailing edge. Reattachment occurs downstream of the maximum pressure gradient, when $C_p \approx -0.3$. Increasing the AoA, causes the reattachment point to move downstream, and the maximum positive pressure gradient decreases.

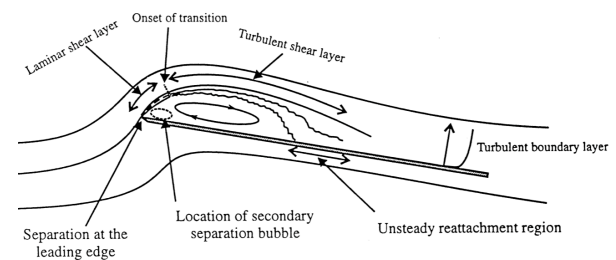


Figure 2: Schematic diagram of the long leading edge bubble from [5].

Pressure Distribution on the Genoa at high AoAs

At AoAs higher than the ideal AoA, the leading edge separation bubble occurs on the leeward side of the genoa. The stagnation point is at the leading edge for all the conditions of interest and, hence, $C_p = 1$ at the leading edge. The pressure shows a minimum near the leading edge, followed by a positive pressure gradient correlated with the reattachment point. Then, the curvature-related suction peak occurs. Therefore, two suction peaks occur: the leading edge suction peak near the leading edge, and the curvature-related suction peak near where the maximum camber of the sail section is located.

When the AoA increases, the leading edge bubble enlarges, the suction peak moves downstream, and the positive pressure gradient related to the reattachment decreases. The trailing edge separation point moves upstream and the curvature-related suction peak decreases.

At high AoAs, the leading edge suction peak, which moves downstream when the AoA increases, overlaps the curvature-related suction peak, which decreases when the AoA increases due to the trailing edge separation. The pressure distribution shows a suction peak in the fore part of the chord, followed by an asymptotic pressure recovery up to the base pressure.

Leading and Trailing Edge Pressures on the Genoa

The pressures on the leeward side and on the windward side of the genoa are equal at the leading edge and at the trailing edge. However, the distances of the closest pressure taps from the leading and the trailing edges (located at roughly 3% and 98% of the chord, respectively) do not allow the leading-edge and the trailing-edge pressures to be measured on either side.

In the present paper, C_p has been assumed to be $C_p = 1$ at the leading edge. In fact, the stagnation point is expected to be at the leading edge of the genoa for all the tested conditions. Indeed, a cross-flow component can occur along the sail span. On the sail, there must be one point where all the flow components are zero and $C_p = 1$, but it does not have to occur along all of the leading edge. Therefore, at the leading edge C_p could be slightly lower than 1.

At the trailing edge of the genoa, C_p is typically negative. It should be reminded that, in inviscid flow, at the trailing edge $C_p = 1$ for thick airfoils, while $C_p = 0$ for infinitely thin profiles. Negative C_p 's are related to separated flow.

At high AoAs, when the trailing edge separation occurs on the leeward side of the sail, the pressure recovery is interrupted when the separation occurs. Therefore, the higher the AoA, the lower the trailing edge pressure.

The lift generated by the mainsail has 2 consequences on the genoa pressure distribution. Firstly, It leads to an AoA increase for the genoa (upwash). In fact, when either the mainsail or the genoa is trimmed in, the measured pressure distribution trend on the genoa is similar. Secondly, the genoa trailing-edge pressure decreases due to the "slot effect" [6], because the trailing edge is in the mainsail suction region. Therefore, if trailing edge separation does not occur, increasing the AWA or trimming in the mainsail, achieves a higher mainsail lift, which leads to lower genoa trailing edge pressure. Conversely, trimming in the genoa leads to a genoa AoA increase and not to a mainsail lift increase. Therefore, the genoa trailing-edge pressure increases, as mentioned in the previous section.

If trailing edge separation does not occur, the pressure coefficient at the trailing edge is typically in the range $0 < C_p < -0.5$.

For instance, Figure 3 shows C_p measured on the mid-high section of the model-scale genoa, at 4 different apparent wind angles (AWA), which is the angle between the longitudinal boat axis and the free-stream velocity. The non-dimensional chord length (x/c) is used on the abscissa. The ideal AoA on the measured section is achieved at AWA=20°.

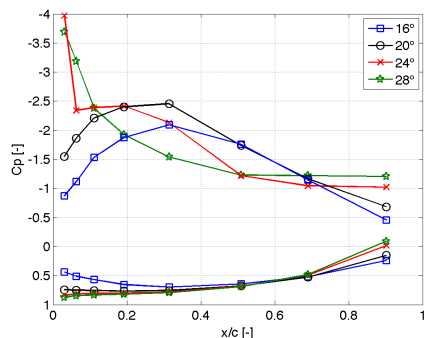


Figure 3: Leeward and Windward C_p s on the model-scale genoa.

Windward Pressure Distribution on the Genoa

The pressure on the sail must always be lower than the stagnation pressure ($C_p = 1$) and, on the windward side of the genoa, is always higher than the trailing edge pressure. At AoAs equal or higher than the ideal AoA, on the windward side of the genoa, an attached boundary layer grows from the leading edge up to the trailing edge.

As mentioned above, in the present work, the leading edge pressure gradient cannot be measured. However, in this region, at the ideal AoA, high pressure gradients are expected. In fact, the flow accelerates downstream of the stagnation point and the pressure decreases suddenly. Further downstream, the sail curvature causes the pressure to increase, reaching a maximum near the maximum sail camber. Then, the pressure decreases to match the leeward side pressure at the trailing edge.

When the AoA is increased, the negative pressure gradient at the leading edge is expected to decrease. In fact, for instance, on a flat plate, the pressure decreases monotonically up to the trailing edge. At $AoA = 1^\circ$, C_p drops from $C_p = 1$ to $C_p \approx 0.2$ in the first 3% of the chord length, then it decreases at low rate until the

trailing edge where $C_p \approx -0.2$. At $AoA = 5^\circ$, $C_p \approx 0.65$ at $x/c = 3\%$.

On the genoa, $C_p = 1$ at the leading edge, then a suction peak occurs in the first 3% of the chord, followed by a curvature-related pressure peak and, finally, by a pressure decrease up to the trailing edge. Increasing the AoA, causes the suction peak to decrease, while the curvature-related pressure peak increases. The higher the AoA, the further upstream the pressure peak occurs. At high AoAs, the leading edge suction peak becomes negligible and the pressure decreases monotonically up to the trailing edge.

On rigid sails, the sail shape does not change when the AoA is lower than the ideal AoA. In these circumstances, the leading edge separation bubble occurs on the windward side. Near the leading edge, the pressure drops down and then increases again until the reattachment point. The pressure can increase even further after the reattachment point due to the sail curvature.

Figure 4 shows the windward C_p measured on the mid-high section of the model-scale genoa, for 4 different genoa trims and two AWAs. The AoA increases when the genoa is tightened (from "J4" to "J1") and also when the AWA is increased (from 16° to 28°). The ideal AoA is achieved by the trim "J2" at AWA=16°.

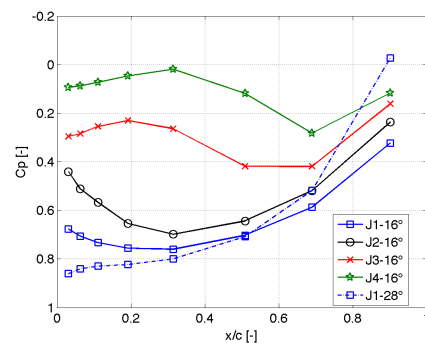


Figure 4: Windward C_p on the model-scale genoa.

Pressure Distribution on the Mainsail

Pressure Distribution on the Leeward Side of Mast/Mainsail

The mast in front of the mainsail affects the flow on the rear part of the mainsail. The stagnation point is located on the mast and its location depends on both the genoa and mainsail trims. On the leeward side, the flow accelerates around the mast curvature and a suction peak occurs. The adverse pressure gradient causes the laminar boundary layer to separate. The laminar shear layer becomes turbulent and reattaches onto the mainsail surface. A low recirculation flow velocity and a low pressure gradient across the bubble are expected. In fact, the backflow is slowed down by the step made of the backward face of the mast. In the present paper pressures on the mast are not measured. Wilkinson [7] measured pressures on a 2D mast/mainsail section. He found that the pressure recovery is interrupted at the separation point. The pressure remains constant up to the laminar to turbulent transition in the rear part of the bubble. Downstream of the reattachment point, the pressure decreases again due to the sail curvature. In the present paper, the first pressure tap on the mainsail is located at around 3% of the chord length, where the pressure is already recovering after the laminar to turbulent transition.

At low AoAs, the leading edge bubble is shorter and the pressure recovery is higher. Positive values up to $C_p = 0.5$ were measured at the first pressure tap. Downstream, suction due to the mainsail curvature occurs, which is significantly lower than the curvature-related suction occurring on the genoa. In fact, the curvature of

the mainsail is lower than the curvature of the genoa. The moderate curvature-related suction makes trailing edge separation less likely to occur.

Increasing the AoA, causes the leading edge suction peak to increase and the positive pressure gradient to decrease. The leading edge bubble enlarges and the maximum pressure occurs further downstream. The curvature-related suction increases with increase in the AoA.

At high AoAs, a monotonic pressure increase occurs. Increasing the AoA, causes it to occur earlier at the lowest mainsail sections where the sail is flatter, and at the highest sections where the curvature-related suction is smoothed due to the trailing edge separation, than at the mid-section.

Leading and Trailing Edge Pressures on the Mast/Mainsail

On mast/mainsail sections, the stagnation point is on the mast. The cross flow velocity along the mast is expected to be negligible and hence, C_p is expected to be exactly $C_p = 1$.

The trailing edge pressure is typically closer to zero for the mainsail than for the genoa. On the mainsail trailing edge C_p is almost $C_p = 0$ at the bottom sections, and decreases from the bottom to the highest sections.

Windward Pressure Distribution on the Mast/Mainsail

Figure 5 shows C_p measured on the mid-high section of the model-scale genoa, for 3 mainsail trims and 2 AWAs. The resulting AoA increases when the mainsail is tightened (from trim “M4” to “M1”) and the AWA is increased (from 16° to 28°).

On the windward side, downstream of the stagnation point on the mast, an attached boundary layer develops. The mast curvature causes the flow to accelerate and a suction peak occurs. The pressure recovery after the peak is too severe for the boundary layer and separation occurs near the suction peak. Laminar to turbulent transition occurs on the separated shear layer, which leads the shear layer to reattach. Reattachment can occur further downstream along the chord than the reattachment on the leeward side of the sail. The recirculation flow has low mean velocity, which leads to a constant pressure along most of the bubble length. Downstream of reattachment, the pressure can increase even further due to the sail curvature, before decreasing at low rate to match the trailing edge pressure.

At low AoAs, the windward leading edge bubble can extend to more than $3/4^{\text{th}}$ of the chord length. On the bottom sections, the low sail curvature causes the reattachment to occur earlier than on the mid sections, where the curvature is higher.

The bubble becomes shorter when the AoA is increased. Both the stagnation point and the separation point on the mast move downstream along the mast, while reattachment occurs closer to the leading edge on the mainsail. The pressure plateau is at a higher pressure, and the positive pressure gradient increases.

At high AoAs, the pressure decreases monotonically from the leading edge to the trailing edge.

Full-scale & Model-scale pressure distributions

No significant differences between the full-scale and the model-scale pressure trends were found. The comparison showed that the dynamic pressure measured in full-scale was probably overestimated by about 30% and, hence, all the full-scale measurements were corrected accordingly. The pressure variations showed consistent trends but it was not possible to estimate the measurement accuracy.

For instance, Figure 6 shows good agreement between the pressure distributions measured on the mainsail in full-scale (FS)

and model-scale (MS) for two mainsail trims (“M1” tight, and “M2” eased).

It is interesting to note that when $C_{p\text{windward}} - C_{p\text{leeward}} < 0$, the shape of the flexible sail tested in full-scale changes, while the rigid model-scale sail does not. However, the full-scale and the model-scale C_p trends are in good agreement.

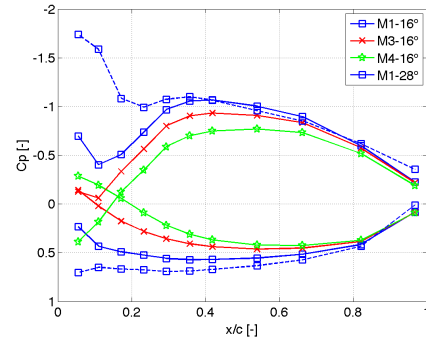


Figure 5: Leeward and Windward C_p 's on the model-scale mainsail.

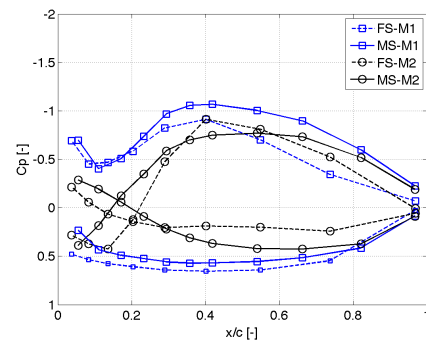


Figure 6: Leeward and Windward C_p 's on the model-scale and full-scale mainsails.

Conclusions

The observed results are in good agreement with the sparse literature on this subject. In particular, they can be explained in terms of conventional aerodynamic theory for thin aerofoils.

There was good agreement between the model and full-scale results in terms of the observed trends.

References

- [1] Crompton MJ & Barret RV, Investigation of the Separation Bubble Formed Behind the Sharp Leading Edge of a Flat Plate at Incidence. *Proc. Inst. of Mech. Eng., Part G: J. of Aerospace Eng.*, 214 (3) 157-176, 2000.
- [2] Fluck M, Gerhardt FC, Pilate J, Flay RGJ, A Comparison of Potential Flow Based and Measured Pressure Distributions Over Upwind Sails, *J. of Aircraft*, IN PRESS.
- [3] Gault DE, An Investigation at Low Speed of the Flow Over a Simulated Flat Plate at Small Angles of Attacks Using Pitot Static and Hot Wire Probes, *NACA TN-3876*, 1957.
- [4] Gentry A, The Aerodynamics of Sail Interaction, Proc. 3rd AIAA Symp. on the Aero/Hydraulics of Sailing, Redondo Beach, CA, 20 Nov. 1971.
- [5] Viola IM & Flay RGJ, Full-scale Pressure Measurements on a Sparkman & Stephens 24-foot Sailing Yacht, *J. Wind Eng. & Ind. Aero.*, in press, doi:10.1016/j.jweia.2010.07.004
- [6] Warner EP, & Ober S, The Aerodynamics of Yacht Sails. *Proc. 3rd General Meeting of the Society of Naval Arch. and Marine Eng.*, New York, 12th -13th Nov. 1925.
- [7] Wilkinson S, Partially Separated Flows Around 2D Masts and Sails, *PhD Thesis*, University of Southampton, 1984.